On L-shaped point set embeddings of trees: first non-embeddable examples*

Torsten Mütze† Manfred Scheucher†

Abstract

An *L-shaped* embedding of a tree in a point set is a planar drawing of the tree where the vertices are mapped to distinct points and every edge is drawn as a sequence of two axis-aligned line segments. There has been considerable work on establishing upper bounds on the minimum cardinality such that any point set of that size admits an L-shaped embedding of any n-vertex tree with maximum degree 4. However, no non-trivial lower bound is known to this date, i.e., no known n-vertex tree requires more than n points to be embedded.

In this paper, we present the first examples of n-vertex trees for $n \in \{13, 14, 16, 17, 18, 19, 20\}$ that require strictly more points than vertices to admit an L-shaped embedding. Moreover, using computer help, we show that every tree on $n \leq 12$ vertices admits an L-shaped embedding in every set of n points.

We also consider embedding *ordered* trees, where the cyclic order of the neighbors of each vertex in the embedding is prescribed. For this setting, we determine the smallest non-embeddable ordered tree on $n = 10$ vertices, and we show that every ordered tree on $n \leq 9$ or $n = 11$ vertices admits an L-shaped embedding in every set of n points. We also construct an infinite family of ordered trees which do not always admit an L-shaped embedding, answering a question raised by Biedl, Chan, Derka, Jain, and Lubiw.

1 Introduction

An *L-shaped* embedding of a tree in a point set is a planar drawing of the tree where the vertices are mapped to distinct points of the set and every edge is drawn as a sequence of two axis-aligned line segments; see Figure 1. Here and throughout this paper, all point sets are such that no two points have the same x- or y-coordinate. The investigation of L-shaped embeddings was initiated in [KS11, FHM+12, DGFF+13]. In particular, di Giacomo et al. [DGFF+13] showed that $O(n^2)$ points are always sufficient to embed any n-vertex tree. Note that an L-shaped embedding requires that the maximum degree of the tree is at most 4. Moreover, if the maximum degree is 2, then the tree is a path and can be embedded greedily on any point set of the same size. Formally, let $f_d(n)$ denote the minimum number N of points such that every n-vertex tree with maximum degree $d \in \{3, 4\}$ admits an L-shaped embedding in every point set of size N.

The second author's master's thesis [Sch15] proposed a method to recursively construct an L-shaped embedding of any n-vertex tree in any point set of size $O(n^{1.58})$ (see also [AHS16]). Biedl et al. [BCD+18] gave a more precise analysis of this method, proving that $f_3(n) = O(n^{1.22})$ and $f_4(n) = O(n^{1.55})$ points are enough. To this date, no lower bound besides the trivial

*A short version of this paper appeared in the Proceedings of the 26th International Symposium on Graph Drawing and Network Visualization [MS18].

†Institut für Mathematik, Technische Universität Berlin, Germany, {muetze,scheucher}@math.tu-berlin.de

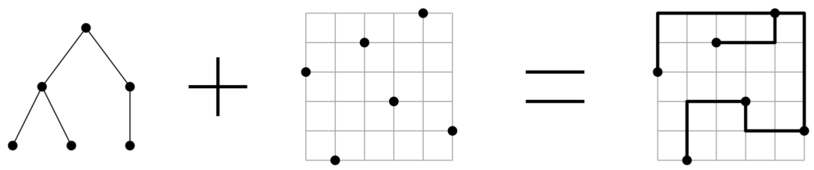

Figure 1: An L-shaped embedding of a tree in a point set.

bound $f_d(n) \geq n$ is known, i.e., no known n-vertex tree requires more than n points to be embedded. Di Giacomo, Frati, Fulek, Grilli, and Krug [DGFF$^+$13] specifically asked for a tree and point set that would prove $f_4(n) > n$. The same question was reiterated by Fink, Haunert, Mchedlidze, Spoerhase, and Wolff [FHM$^+$12], and by Biedl, Chan, Derka, Jain, and Lubiw [BCD$^+$18]. Kano and Suzuki [KS11] even conjectured that $f_3(n) = n$.

However, Biedl et al. [BCD$^+$18] also considered a more restricted setting of embedding *ordered* trees, where the cyclic order of the neighbors of each vertex in the embedding is prescribed. They presented a single 14-vertex ordered tree which does not admit an L-shaped embedding in a particular point set of size 14[1], and they raised the problem to find an infinite family of such non-embeddable ordered trees.

1.1 Our results

We begin presenting our results for the setting where there are no constraints on the cyclic order in which the neighbors appear around each vertex of the tree. With brute-force computer search, we verified that all trees on $n \leq 12$ vertices can be embedded in every point set of size n.

Theorem 1 (Computer-based)**.** *Every tree on $n \leq 12$ vertices admits an L-shaped embedding in every set of n points.*

We also formulated a SAT instance to test a given pair of tree and point set for embeddability. This way, we found a 13-vertex tree that does not admit an embedding in a particular point set.

Theorem 2. *The tree T_{13} in Figure 2 does not admit an L-shaped embedding in the point set S_{13} shown in the figure.*

Even though the 13-vertex tree T_{13} was found using the help of a SAT solver, a human-verifiable proof of Theorem 2 is not hard to obtain.

Besides the pair (T_{13}, S_{13}), we also found pairs of trees and point sets that do not admit an embedding for larger values of n. Overall, we found pairs of n-vertex trees and point sets of size n for $n \in \{13, 14, 16, 17, 18, 19, 20\}$. For $n = 15$, however, our computer search did not yield any non-embeddable example (the search was not exhaustive). We remark that all known non-embeddable trees contain T_{13} as a subtree.

We now focus on the more restricted setting of ordered trees introduced in [BCD$^+$18], where the cyclic order of the neighbors of each vertex in the embedding is prescribed.

Theorem 3 (Computer-based)**.** *Every ordered tree on $n \leq 9$ vertices or on $n = 11$ vertices admits an L-shaped embedding in every set of n points.*

[1] Specifically, their counterexample is the 14-vertex caterpillar with 6 vertices on the central path and a pending edge on each side of the four inner vertices of the path. The point set is a $(4, 6, 4)$-staircase in our terminology (see Definition 5).

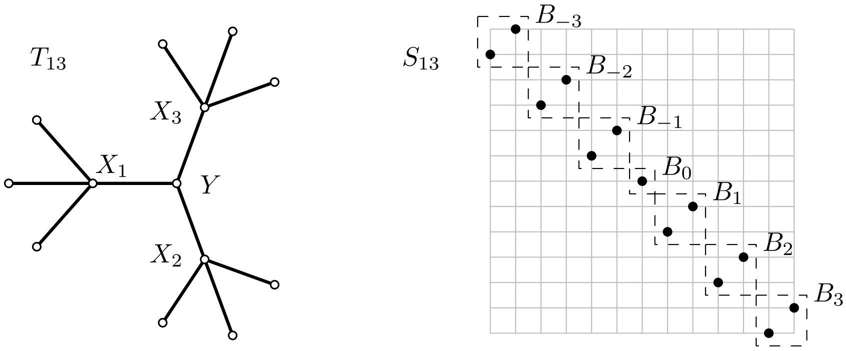

Figure 2: The tree T_{13} (left) does not admit an L-shaped embedding in the $(2, 2, 2, 1, 2, 2, 2)$-staircase point set S_{13} (right). The boxes $B_{-3}, \ldots, B_3$ are highlighted by dashed frames.

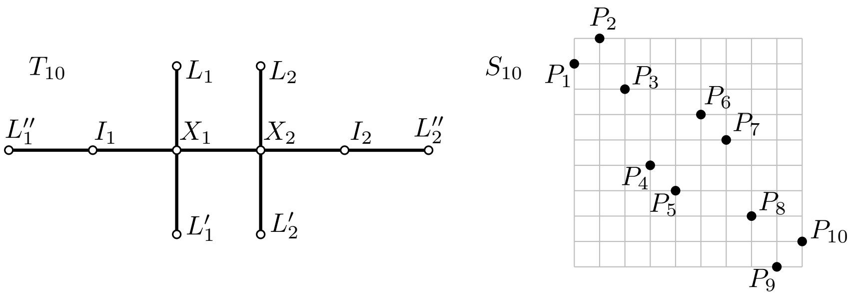

Figure 3: The ordered tree T_{10} (left) does not admit an L-shaped embedding in the point set S_{10} (right).

We also found a 10-vertex tree that does not admit an embedding in a particular point set. This is a smaller non-embeddable instance than the one for $n = 14$ previously presented in [BCD+18].

Theorem 4. *The ordered tree T_{10} in Figure 3 does not admit an L-shaped embedding in the point set S_{10} shown in the figure.*

Remarkably, the pair (T_{10}, S_{10}) is the only one on $n = 10$ vertices/points not admitting an L-shaped embedding.

Moreover, we construct an infinite family of ordered trees that do not admit an L-shaped embedding on certain point sets, answering a question raised by Biedl, Chan, Derka, Jain, and Lubiw in [BCD+18]. As it turns out, the point sets that appear to be difficult for embedding have a regular staircase shape as shown in Figure 4 (see also Figure 2).

Definition 5 (Staircase point set)**.** *For a partition $n = a_1 + \cdots + a_k$ with $k, a_1, \ldots, a_k \in \mathbb{N}$, the* $(a_1, \ldots, a_k)$-staircase *is the point set consisting of a sequence of k boxes, ordered from top-left to bottom-right, and the ith box contains a sequence of a_i points with increasing x- and y-coordinate.*

Theorem 6. *For any even $r \geq 10$, the ordered tree T^*_r on $n = 9r + 8$ vertices in Figure 4 does not admit an L-shaped embedding in the n-point $(2, \ldots, 2)$-staircase.*

We conjecture that T^*_r does not admit an embedding in the same point set, even when considered as an unordered tree, i.e., in the original unrestricted setting.

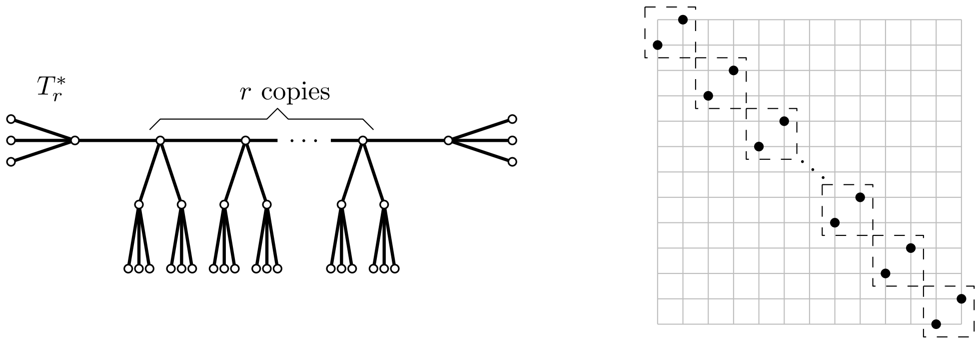

Figure 4: The family of ordered trees T_r^* (left) does not admit an L-shaped embedding in the n-point $(2,\dots,2)$-staircase (right), where $n = 9r + 8$. The boxes of the point set are highlighted.

1.2 Related work

Besides the problem of finding L-shaped embeddings of arbitrary trees in arbitrary point sets, various special classes of trees and point sets have also been studied. For instance, perfect binary and perfect ternary n-vertex trees can be embedded in any point set of size $O(n^{1.142})$ or $O(n^{1.465})$, respectively [BCD$^+$18]. Moreover, trees with pathwidth k can be embedded in any set of $2^k n$ points [Sch15, Chapter 3.3.2] (see also [AHS16]).[2] Specifically, any n-vertex caterpillar with maximum degree 3 can be embedded in any point set of size n [DGFF$^+$13]. A *caterpillar* is a tree with the property that all leaves are in distance 1 of a central path. For maximum degree 4 caterpillars, the currently best known upper bound is $4n/3 + O(1)$ many points [Sch15, Chapter 5.2.1]. Biedl et al. [BCD$^+$18] showed that any ordered caterpillar can be embedded in any point set of size $O(n \log n)$.

When point sets are chosen uniformly at random, i.e., the y-coordinates are a random permutation, it is known that $O(n \log n (\log \log n)^2)$ and $O(n^{1.332})$ points are sufficient to embed any tree with maximum degree 3 or 4, respectively, with probability at least 1/2 [Sch15, Chapter 4] (see also [AHS16]).

Another known setting are non-planar L-shaped point set embeddings, where L-shaped edges are allowed to cross properly, but edge-segments must not overlap. For this setting, it is known that n points are sufficient to embed any n-vertex tree with maximum degree 3 [FHM$^+$12, DGFF$^+$13] or any n-vertex caterpillar with maximum degree 4 [Sch15, Theorem 21]. For n-vertex trees with maximum degree 4 the currently best upper bound on the required number of points is $7n/3 + O(1)$ [Sch15, Theorem 7].

1.3 Outline of this paper

In Sections 2 and 3 we present the proofs of Theorems 2 and 4, respectively. Section 4 is devoted to proving Theorem 6. We describe our computational approach to proving Theorems 1 and 3 by exhaustive search in Section 5. More non-embeddable small trees are presented in Section 6, together with our SAT model which is used to verify non-embeddability. We conclude in Section 7 with some challenging open problems.

[2] For the definition of pathwidth, we refer the reader to [RS83].

2 Proof of Theorem 2

Consider the (unordered) tree T_{13} and the $(2,2,2,1,2,2,2)$-staircase point set S_{13} depicted in Figure 2. We label the degree 3 vertex of T_{13} by Y and the three degree 4 vertices of T_{13} as X_1, X_2, X_3, respectively. Moreover, we label the boxes in the staircase point set S_{13} from left to right by $B_{-3}, B_{-2}, \ldots, B_3$. Note the symmetry of T_{13}, as the vertex Y joins three isomorphic subtrees. Moreover, S_{13} has reflection symmetries along both diagonals of the grid.

For the sake of contradiction, we assume that an L-shaped embedding of T_{13} in S_{13} exists. We first derive three lemmas that capture to which boxes the vertices X_1, X_2, X_3, Y can be mapped in such an embedding, and we then complete the proof by distinguishing two main cases.

Lemma 7. *Neither of the four vertices X_1, X_2, X_3, Y is mapped to B_{-3} or to B_3.*

Proof. All points in B_{-3} and B_3 lie on the bounding box of the point set, so if one of the X_i is mapped to such a point, then one of the four edges incident with X_i would leave the bounding box, which is impossible. Moreover, Y cannot be mapped to one of these two boxes, as otherwise one of the X_i, which are the only neighbors of Y in T_{13}, would be mapped to the other point of that same box. □

Lemma 8. *Each of the degree-4 vertices X_i is mapped to a distinct box.*

Proof. Assume that X_i and X_j are mapped to the same box. By symmetry, we may assume that X_j is right above X_i, and that Y is right below of X_i and X_j; see Figure 5(a). Note that the edge YX_i enters X_i from below and the edge YX_j enters X_j from the right. As X_i and X_j both have degree 4, and their box only contains two points, the edge leaving X_i to the right and the edge leaving X_j to the bottom must cross, a contradiction. □

(a) (b)

Figure 5: Illustration of the proofs of (a) Lemma 8 and (b) Lemma 9. Crossing edges are highlighted.

Lemma 9. *Not all three points X_1, X_2, X_3 lie on the same side (above, below, left, or right) of Y.*

Proof. It suffices to prove one of the statements, then the others follow by symmetry. Suppose for the sake of contradiction that X_1, X_2, X_3 all lie above Y. As one edge leaving Y has to go right, one of the X_i, say X_3, is mapped to the same box, and Y is left below of X_3 in that box; see Figure 5(b). Moreover, YX_3 is an $\lrcorner$-edge. As X_3 has degree 4, and each box contains at most two points, the edge leaving Y on the top towards X_1 or X_2 crosses the edge that leaves X_3 to the left, a contradiction. □

By Lemma 7 and Lemma 9, Y is mapped to one of the boxes B_{-1}, B_0, or B_1. By Lemma 8 we may assume that X_1, X_2, X_3 appear in distinct boxes in exactly this order from left to right and also from top to bottom, and none of them is in B_{-3} or B_3. Moreover, from Lemma 9 we conclude that X_1 and X_3 are in other boxes than Y, so at most Y and X_2 are in the same box. We now distinguish two cases.

Case 1: Y and X_2 are mapped to the same box. By symmetry, we may assume that they are mapped to B_1 and that X_2 lies right above Y. Then the vertex X_3 must be mapped to the box B_2; see Figure 6(a). If YX_3 would be a $\urcorner$-edge, then it would cross the edge leaving X_2 at the bottom. It follows that YX_3 is a $\llcorner$-edge. Note that the edge that leaves X_2 to the right can only connect to a leaf L that is mapped to $B_2 \cup B_3$, and L must be mapped to the right of X_3, as otherwise the edges X_2L and YX_3 would cross. The edges leaving X_3 at the bottom and right can only connect to points from $B_2 \cup B_3$, so together with X_3 and L we already have four vertices that are mapped to $B_2 \cup B_3$. Consequently, the edge leaving X_3 at the top must connect to a point outside of $B_1 \cup B_2 \cup B_3$, and therefore this edge crosses the edge X_2L, a contradiction.

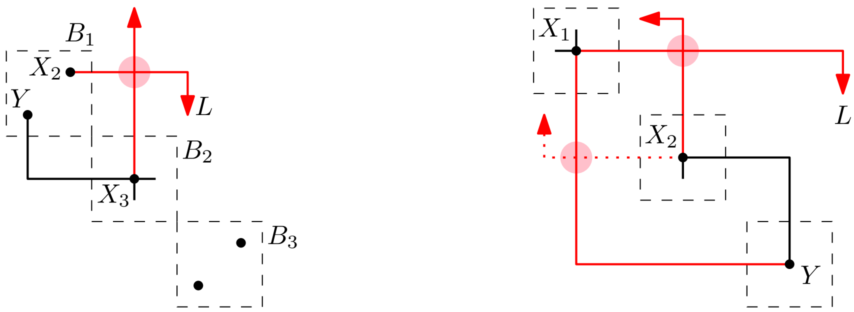

(a) Case 1 (b) Case 2

Figure 6: Illustration of the proof of Theorem 2.

Case 2: Y and X_2 are mapped to distinct boxes, so all four points X_1, X_2, X_3, Y are in different boxes. By symmetry, we assume that X_1 and X_2 both lie above and left of Y, and X_3 lies below and right of Y. Moreover, we assume that YX_1 us a $\llcorner$-edge and that YX_2 is a $\urcorner$-edge; see Figure 6(b). Note that X_2 cannot connect to any points right of Y, and X_1 can only connect to such points by the edge leaving it to the right. As Y is either mapped to B_0 or B_1, there are at most 7 points left above of Y. Therefore, as X_1 and X_2 together with their leaves form a set of 8 points, Y must be mapped to B_1, and exactly one leaf L of X_1 is mapped to a point right of Y, connected to X_1 via a $\urcorner$-edge. Note that X_2 cannot be mapped to B_0, as then the edge leaving X_2 at the bottom could not connect to any point without either crossing YX_1 or YX_2. Consequently, X_2 is mapped to B_{-1}. However, as B_{-1} and B_0 together contain only 3 points, and X_2 together with its leaves form a set of 4 vertices, at least one of the two edges that leave X_2 to the left or top must connect to a point above or left of X_1, and this edge will cross either the edge YX_1 or X_1L, again a contradiction.

In both cases we obtain a contradiction to the assumption that T_{13} admits an L-shaped embedding in the point set S_{13}. This completes the proof of Theorem 2.

3 Proof of Theorem 4

Consider the ordered tree T_{10} and the point set S_{10} depicted in Figure 3. We label the two degree 4 vertices of T_{10} by X_1, X_2 and the two degree 2 vertices by I_1, I_2. Moreover, we label the leaves adjacent to X_1 and X_2 by L_1, L_1', L_2, L_2', and the leaves adjacent to I_1 and I_2 by L_1'' and L_2'', as shown in the figure. We label the points of the point set S_{10} from left to right by $P_1, \ldots, P_{10}$. Note the symmetry of T_{10}, and observe that S_{10} has reflection symmetries along both diagonals of the grid.

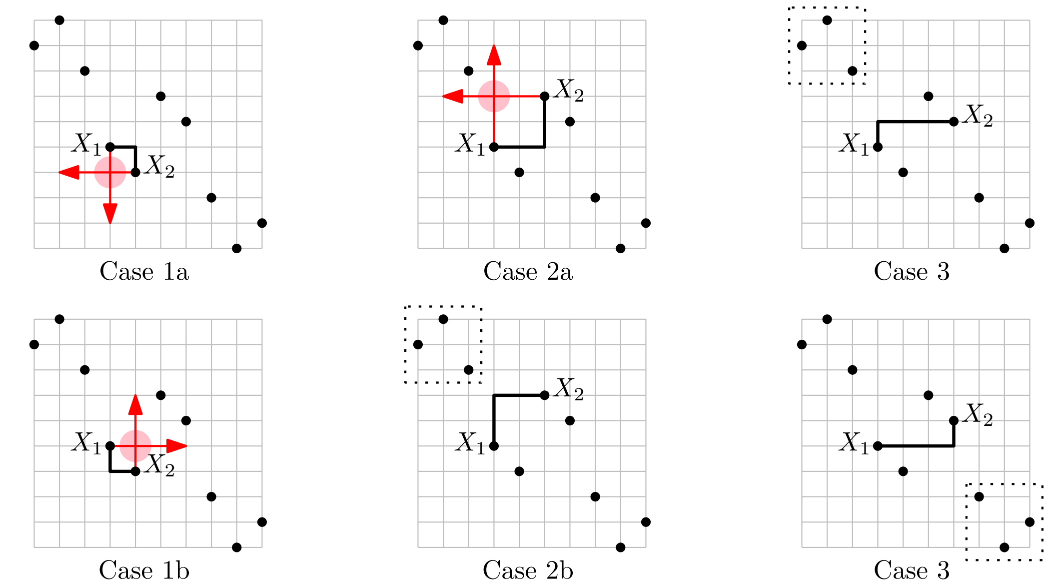

Figure 7: Illustration of the proof of Theorem 4.

For the sake of contradiction, we assume that an order-preserving L-shaped embedding of T_{10} in S_{10} exists. Clearly, none of the degree 4 vertices X_1, X_2 can be mapped to any of the four points P_1, P_2, P_9, P_{10} which lie on the bounding box of the point set S_{10}. We also claim that X_1, X_2 cannot be mapped to P_3 or P_8. By symmetry, it suffices to exclude the case that X_1 is mapped to P_3. In this case, we may assume by symmetry that X_2 is connected to X_1 from the right. Consequently, due to the cyclic order of the neighbors of X_1, I_1 must be mapped to P_1 and L_1 must be mapped to P_2. Then L_1'' cannot be mapped to any point, a contradiction.

It follows that X_1 and X_2 are mapped to one of the points P_4, P_5, P_6, P_7. By symmetry, we may assume that X_1 is mapped to P_4. We now distinguish six cases, illustrated in Figure 7:

- Case 1a: X_2 is mapped to P_5 and X_1X_2 is a ⌝-edge. In this case, the edge leaving X_1 at the bottom and the edge leaving X_2 to the left must cross, a contradiction.
- Case 1b: X_2 is mapped to P_5 and X_1X_2 is a ⌞-edge. In this case, the edge leaving X_1 to the right and the edge leaving X_2 to the top must cross, a contradiction.
- Case 2a: X_2 is mapped to P_6 and X_1X_2 is a ⌟-edge. In this case, the edge leaving X_1 to the top and the edge leaving X_2 to the left must cross, a contradiction.
- Case 2b: X_2 is mapped to P_6 and X_1X_2 is a ⌜-edge. Clearly, none of the four vertices L_1', L_2', I_1, and I_2 can be mapped to P_1, P_2, or P_3. We claim that L_1'' and L_2'' cannot be mapped to any of these points either. Indeed, X_1I_1 is an ⌞-edge, and I_1 can only be mapped to one of P_5, P_8, P_9, or P_{10}. If L_1'' is mapped to one of P_1, P_2, or P_3, then I_1 and L_1'' must be joined via an ⌝-edge and either the first of the two edges X_1I_1 and I_1L_1'' intersects the edge X_1X_2 or these two edges prevent one or both of the points P_9, P_{10} from being reachable from X_2 via one or two L-shaped edges. Consequently, only two vertices, namely L_1 and L_2 can be mapped to the three points P_1, P_2, P_3, a contradiction.
- Case 3: X_2 is mapped to P_7. The subcases where X_1X_2 is an ⌜-edge or an ⌟-edge are symmetric, so it suffices to consider the first one. In this case we can argue as in Case 2b that only L_1 and L_2 can be mapped to the three points P_1, P_2, P_3, a contradiction.

In each case we obtain a contradiction, so this completes the proof of Theorem 4.

4 Proof of Theorem 6

We label the degree 4 vertices of the ordered tree T_r^* along the central path by $X_0, \dots, X_{r+1}$, and for any vertex X_i, $1 \le i \le r$, we label its two neighbors of degree 4 not on the central path by X_i' and X_i'', as shown in Figure 8. For our later arguments it will be convenient to orient the edges of T_r^* which are not on the central path. Edges incident to a leaf are oriented away from the leaf and edges $X_i'X_i$ and $X_i''X_i$ are oriented towards X_i.

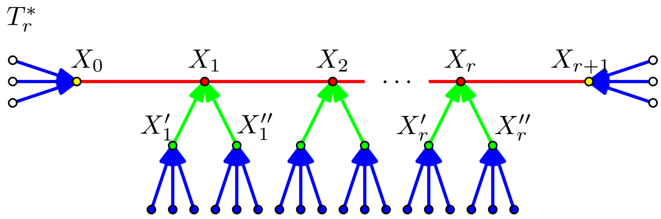

Figure 8: Labeling of vertices of the ordered tree T_r^* for the proof of Theorem 6.

Lemma 10. *Each of the degree-4 vertices X_i, X_i', and X_i'' is mapped to a distinct box of the n-point $(2, \dots, 2)$-staircase.*

Proof. Assume that two degree 4 vertices P, Q of T_r^* are mapped to the same box, such that Q is right above P. As P and Q have degree 4, there are edges in all four directions leaving both P and Q. The edges leaving P to the top and Q to the left, or the edges leaving P to the right and Q to the bottom will cross, unless one pair of them forms a single L-shaped edge, which may happen only if P and Q are neighbors in the tree. In any case, at least the remaining pair of edges must cross, a contradiction. □

We refer to the sequence of ⌝- or ⌞-edges connecting the central path vertices $X_0, \dots, X_{r+1}$ as the *spine*. By symmetry, we may assume w.l.o.g. that X_0 is mapped to a box left of X_1. In the following we distinguish two main cases, depending on whether X_0X_1 is an ⌝-edge or an ⌞-edge.

4.1 Case 1: X_0X_1 is an ⌝-edge

Throughout this section, we assume that X_0X_1 is an ⌝-edge. Lemma 10 and the cyclic order of neighbors around each of the vertices X_i, $i = 0, \dots, r+1$, now enforce a particular shape of all tree edges that connect two degree-4 vertices, as captured by the following lemma; see Figure 9.

Lemma 11. *The vertices $X_0, \dots, X_{r+1}$ appear exactly in this order from left to right, and any two consecutive such vertices are connected by an ⌝-edge. Moreover, for $i = 1, \dots, r$,*

- *the vertices X_i' and X_i are connected by an ↳-edge;*
- *the vertices X_i'' and X_i are connected by an ↰-edge;*
- *the three edges directed from the leaves towards the vertices X_i', X_i'', X_0, and X_{r+1} form a ⊹, ⊹, ⊹, and ⊹, respectively.*

By Lemma 10, each box containing one of the X_i, $1 \le i \le r$, contains a second point to which a leaf is mapped. We denote this point by P_i. Combining Lemmas 10 and 11 yields the following lemma, which is illustrated in Figure 10.

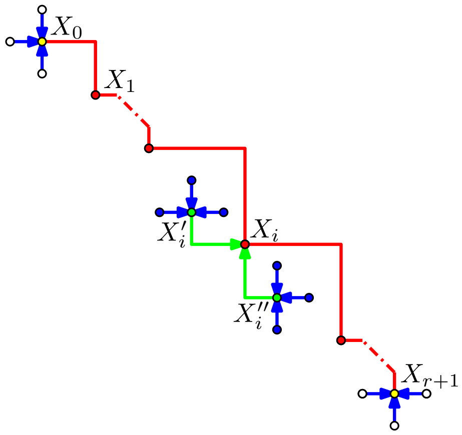

Figure 9: Illustration of Lemma 11.

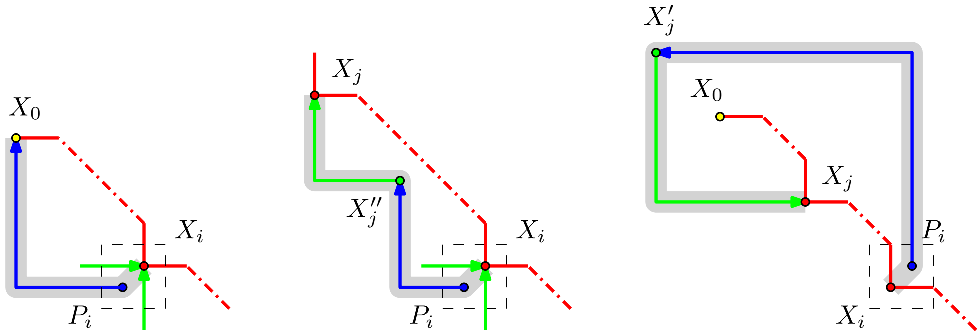

Figure 10: Illustration of Lemma 12. The corresponding ⬑-, ⬏-, and ⮒-blockers are highlighted with bold lines.

Lemma 12. *For every point P_i below the spine exactly one of the following four conditions holds:*

- *P_i is connected to X_0 by an ⬑-edge;*
- *P_i is connected to X_{r+1} by an ↳-edge;*
- *there is an index j, $1 \leq j < i$, such that P_i, X''_j, X_j are joined by two consecutive ⬑-edges;*
- *there is an index j, $i < j \leq r$, such that P_i, X'_j, X_j are joined by two consecutive ↳-edges.*

For every point P_i above the spine exactly one of the following two conditions holds:

- *there is an index j, $1 \leq j \leq r$, such that P_i, X'_j and X'_j, X_j are joined by an ↰-edge and an ↳-edge, respectively, wrapping around the top left end of the spine;*
- *there is an index j, $1 \leq j \leq r$, such that P_i, X''_j and X''_j, X_j are joined by an ⬎-edge and an ⬑-edge, respectively, wrapping around the bottom right end of the spine.*

Consider any pair of points P_i, X_0 as in Lemma 12 connected by an ⬑-edge. We refer to this edge together with the short diagonal line joining the points X_i and P_i in the same box (this line is not part of the tree embedding), as a *⬑-blocker starting at X_i and ending at X_0*, see Figure 10. Similarly, given any triple of points P_i, X''_j, X_j as in Lemma 12 joined by two consecutive ⬑-edges, we refer to these two edges together with the line joining X_i and P_i, as a *⬏-blocker starting at X_i and ending at X_j*. Moreover, given any triple of points P_i, X'_j, X_j as in

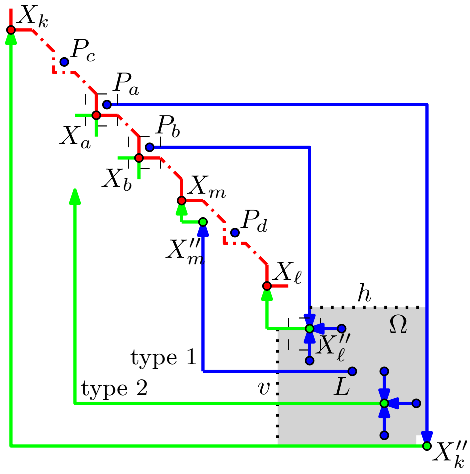

Figure 11: Illustration of Lemma 13.

Lemma 12 joined by a ↰-edge followed by ↳-edge wrapping around the top left end of the spine, we refer to these two edges together with the line joining X_i and P_i, as a ⮌-*blocker starting at* X_i *and ending at* X_j. The terms ↳-*blocker*, ↴-*blocker* and ⮎-*blocker* are defined analogously. Observe that no other tree edge can cross a blocker.

For every index i_1, $1 \le i_1 \le r$, we define a finite sequence of blockers as follows: For $j = 1, 2, \ldots$ we consider the point X_{i_j} and the blocker starting at X_{i_j}. The endpoint $X_{i_{j+1}}$ of this blocker defines the next index i_{j+1}. If $i_{j+1} \notin \{i_1, \ldots, i_j\} \cup \{0, r+1\}$, we repeat this process, otherwise we stop. This yields a finite sequence of indices $i_1, i_2, \ldots, i_\ell$, such that any two consecutive points X_{i_j} and $X_{i_{j+1}}$ are joined by a blocker starting at X_{i_j} and ending at $X_{i_{j+1}}$. Moreover, we either have $i_\ell \in \{i_1, \ldots, i_{\ell-1}\}$ if the blockers close cyclically, or $i_\ell \in \{0, r+1\}$ if the last blocker ends at X_0 or X_{r+1} (the terminal index is included in the sequence). We refer to the sequence of blockers generated in this fashion as the *blocker sequence starting at* X_{i_1}.

The statement and proof of the following key lemma are illustrated in Figure 11.

Lemma 13. *Let* $1 \le a < b \le r$ *be such that* P_a *and* P_b *are two consecutive points above the spine both contained in a* ⮎*-blocker, and let* X_k *and* X_ℓ *be the blocker endpoints, respectively. Then there are indices* c, d *with* $k < c < d \le \ell$ *such that* P_c *and* P_d *are above the spine. Symmetrically, if* P_a *and* P_b, $1 \le a < b \le r$, *are two consecutive points above the spine both contained in a* ⮌*-blocker, then there are indices* c, d *with* $k \le c < d < \ell$ *such that* P_c *and* P_d *are above the spine.*

Observe that this lemma does not make any assertions about the relative positions of the points in $\{X_a, X_b\}$ and $\{X_k, X_\ell\}$. In particular, it does not make any assertions about the disjointness of the sets $\{P_a, P_b\}$ and $\{P_c, P_d\}$.

Proof. It suffices to prove the first part of the lemma where P_a and P_b are both contained in a ⮎-blocker. The second part follows by symmetry. Let h denote the horizontal line segment slightly above the box containing X''_ℓ between the two vertical segments of the ↴-edges leaving P_a and P_b. Let v denote the vertical line segment slightly left of the box containing X''_ℓ between the two horizontal segments of the ↵-edges leaving X''_k and X''_ℓ. Let Ω denote the region enclosed by the two ⮎-blockers starting at X_a and X_b and between the segments h and v, without the point X''_k. Note that Ω contains X''_ℓ and also the second point in its box, but neither X''_k nor the second point in its box, so Ω contains an even number of points from the $(2,\ldots,2)$-staircase. Observe also that no edge crosses the segment h, as P_a and P_b are consecutive points above the spine. Consider an edge crossing the segment v. By Lemma 11, this can only be an ↰-edge starting at a leaf L in Ω and ending at a vertex X''_m for some m, $k < m < \ell$ (type 1), or an ↰-edge starting at some X''_m in Ω, $k < m < \ell$, and ending at X_m (type 2). Figure 11 gives an illustration of both types of edges. In the case of a type 2 edge as before, all three leaves adjacent to X''_m must also be in Ω. Therefore, every type 1 edge contributes 1 to the number of vertices in Ω, and every type 2 edge contributes 4 to the number of vertices in Ω. Note that the other two leaves adjacent to X''_ℓ apart from P_b must also be in Ω, so X''_ℓ together with these two leaves contributes 3 to the number of vertices in Ω. As the number of points from the $(2,\ldots,2)$-staircase in Ω is even, there must be at least one type 1 edge starting at a leaf L in Ω and ending at a vertex X''_m, $k < m < \ell$.

By Lemma 11, X''_m is connected to X_m by another ↰-edge. Now consider the blocker sequence starting at X_m. We prove that it must contain a ⮣-or ⮠-blocker. For the sake of contradiction suppose not. Then it can only have ⬑-blockers, but no ↰-, ↳-, or ⬎-blockers: Indeed, an ↰-blocker would lead to X_0, which is impossible because of the ↰-edge between X''_k and X_k that shields this blocker sequence from the left. Moreover, an ↳- or ⬎-blocker would force one of the points X_i, $1 \leq i \leq r+1$, to lie inside Ω, which is impossible. However, if the blocker sequence consists only of ⬑-blockers, then it must end at X_0, which is again impossible. This proves our claim that the blocker sequence starting at X_m contains a ⮣- or ⮠-blocker, and the first such blocker in the sequence will contain the desired point P_c, $k < c \leq m$ (if the very first blocker is of this type then $c = m$).

An analogous argument applies to the blocker sequence starting at X_ℓ. As the ↰-edge between L and X''_m shields this blocker sequence from the left, the first ⮣- or ⮠-blocker in this sequence contains the desired point P_d, $m < d \leq \ell$. This completes the proof of the lemma. □

We will later use the following corollary of Lemma 13.

Corollary 14. *Suppose there are $\alpha \geq 2$ points $P_{i_1},\ldots,P_{i_\alpha}$, $i_1 < \cdots < i_\ell$, above the spine all contained in a ⮠-blocker, and let X_k be the endpoint of the blocker starting at X_{i_1}. Then we have $k < i_1$, and there are at least $2(\alpha-1)$ many points P_i with $i > k$ above the spine. Symmetrically, suppose there are $\alpha \geq 2$ points $P_{i_1},\ldots,P_{i_\alpha}$, $i_1 < \cdots < i_\ell$, above the spine all contained in a ⮣-blocker, and let X_k be the endpoint of the blocker starting at X_{i_α}. Then we have $k > i_\alpha$, and there are at least $2(\alpha-1)$ many points P_i with $i < k$ above the spine.*

Proof. Apply Lemma 13 to any pair of consecutive points above the spine that are both contained in a ⮠- or ⮣-blocker. □

Consider the collection of all blocker sequences starting at any of the points X_i, $1 \leq i \leq r$. Any blocker in one of these sequences encloses a region together with the spine, and if this region touches a spine edge from the bottom left, then we say that this spine edge is *enclosed.* Any spine edge that is not enclosed is called *free.* In Figure 12, enclosed regions are shaded. For any point A of the staircase point set, consider the second point A' in the same box of the staircase, and let $L(A)$ denote the halfplane containing those two points, such that the points lie slightly to the left of the boundary of the halfplane. We define the halfplane $R(A)$ analogously, by changing left and right in the previous definition.

Lemma 15. *There is no valid embedding of T^*_r with zero or one free spine edges.*

Proof. We choose two particular degree 4 vertices A and B of T^*_r as follows: If there are no ⮣-blockers, then $A := X_0$, and otherwise A is defined as the middle vertex of the outermost

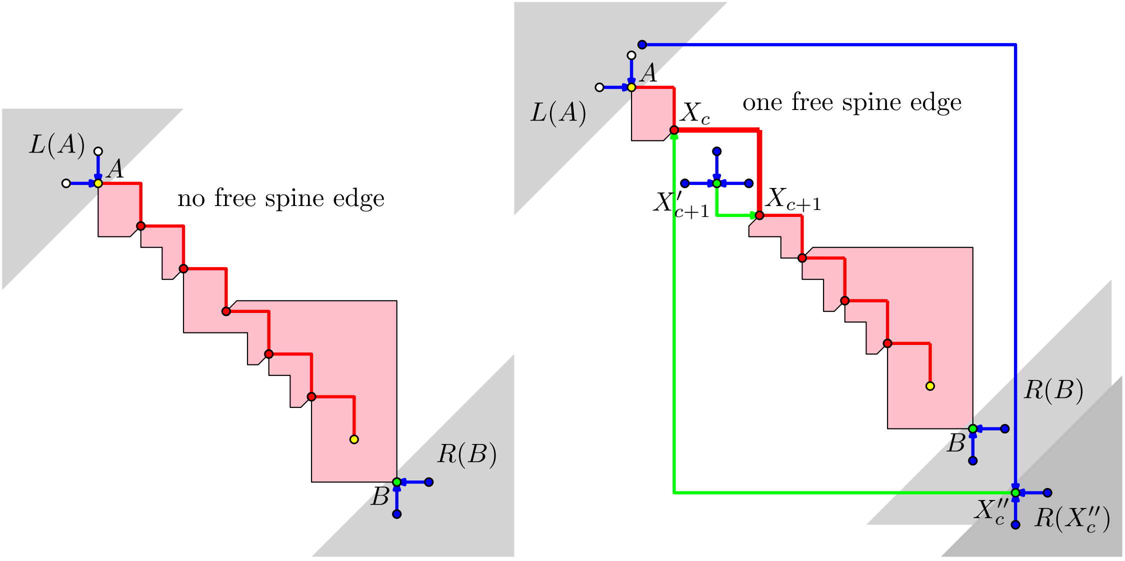

Figure 12: Illustration of Lemma 15. Regions enclosed by blockers and the spine are shaded.

⬏-blocker. Similarly, if there are no ⬎-blockers, then $B := X_{r+1}$, and otherwise B is defined as the middle vertex of the outermost ⬎-blocker; see Figure 12. Note that if $A = X_0$ and the spine edge X_0X_1 is enclosed, then the edge entering X_0 from the bottom is part of a ↰-blocker. Similarly, if $B = X_{r+1}$ and the spine edge X_rX_{r+1} is enclosed, then the edge entering X_{r+1} from the left is part of a ↳-blocker.

We first assume that there is no free spine edge. Consider the regions $L(A)$ and $R(B)$. Note that A and exactly two of the leaves adjacent to it lie in $L(A)$, and that B and exactly two of the leaves adjacent to it lie in $R(B)$. On the other hand, both regions contain an even number of points from the $(2, \ldots, 2)$-staircase. This immediately yields a contradiction, as none of the vertices X'_i, X''_i, $1 \leq i \leq r$, or any of the leaves adjacent to them can reach into $L(A)$ or $R(B)$; see the left hand side of Figure 12.

It remains to consider the case that there is one free spine edge X_cX_{c+1}, $0 \leq c \leq r$. In the following we only consider the subcase $1 \leq c \leq r-1$; see the right hand side of Figure 12. The remaining subcases $c = 0$ and $c = r$ are symmetric, and can be handled analogously. We again consider the regions $L(A)$ and $R(B)$. As X_cX_{c+1} is the only free spine edge, at least one of the vertices X''_c, X'_{c+1} or one of the leaves adjacent to one of them must also be inside $L(A)$ and $R(B)$. By symmetry, we may assume that the ↰-edge from X''_c to X_c or the ↰-edge entering X''_c has its starting point in $R(B)$. This prevents the ↳-edge from X'_{c+1} to X_{c+1} or the ↳-edge entering X'_{c+1} from reaching into $L(A)$. In this situation the starting point of the ⬎-edge entering X''_c is the only one that can reach into $L(A)$, wrapping around the entire spine, which forces X''_c to be in $R(B)$. This, however, leads to a contradiction, as only 3 vertices would be mapped to points in $R(X''_c)$. □

With Corollary 14 and Lemma 15 in hand, we are ready to complete the proof of Theorem 6 in the case that X_0X_1 is an ⬎-edge. We let α_L and α_R denote the number of the number of points P_i above the spine that are contained in a ⬏ or ⬎-blocker, respectively. Clearly, $\alpha := \alpha_L + \alpha_R$ is the total number of points P_i above the spine. Moreover, when considering the points P_i above the spine from left to right, then we first encounter all those are contained in a ⬏-blocker, and then all those contained in a ⬎-blocker. By symmetry we may assume that $\alpha_L \leq \alpha_R$. In the following we distinguish the five cases $\alpha \in \{0, 1, 2, 3, 4\}$ and the case $\alpha > 4$, and we show that none of them can occur.

Case $\alpha = 0$**:** We claim that in this case, exactly one of the spine edges X_cX_{c+1}, $0 \leq c \leq r$, is free. Specifically, if $c \geq 1$, then the blocker sequence starting at X_c ends at X_0 and encloses the edges X_iX_{i+1}, $0 \leq i < c$, and if $c < r$, then the blocker sequence starting at X_{c+1} ends at X_{r+1} and encloses the edges X_iX_{i+1}, $c < i \leq r$. Applying Lemma 15 will therefore conclude the proof.

To verify this claim, we consider the blocker sequence starting at X_1, which contains only ↰-, ↳-, ⬑- and ↴-blockers, but no ↱- or ↲-blockers (in fact, ⬑-blockers cannot occur either). It either ends at X_{r+1}, and then the claim holds, or it ends at X_0. In the latter case, consider the point X_c, $1 \leq c \leq r$, with highest index reached by this blocker sequence. Clearly, the blocker sequence starting at X_c is a subsequence of the previous sequence, so it ends at X_0 and encloses the spine edges X_iX_{i+1}, $0 \leq i < c$. Moreover, the edge X_cX_{c+1} is free, and if $c < r$, then the blocker sequence starting at X_{c+1} must end at X_{r+1}, enclosing the edges X_iX_{i+1}, $c < i \leq r$.

Case $\alpha = 1$**:** By symmetry we may assume that $\alpha_L = 0$ and $\alpha_R = 1$. Let P_a be the unique point above the spine, i.e., P_a is contained in a ↲-blocker. Consider the blocker sequence starting at X_a. It either ends at X_0, enclosing all spine edges X_iX_{i+1}, $0 \leq i \leq r$, and then we are done with the help of Lemma 15. Otherwise this blocker sequence ends at X_a, enclosing the spine edges X_iX_{i+1}, $a \leq i \leq r$. By considering the blocker sequence starting at X_1, we conclude that in this remaining case there is exactly one free spine edge X_cX_{c+1}, $0 \leq c < a$. Again we are done with the help of Lemma 15.

Case $\alpha = 2$**:** We only need to consider the cases $(\alpha_L, \alpha_R) = (1, 1)$ and $(\alpha_L, \alpha_R) = (0, 2)$. Let P_a, P_b, $a < b$, be the two points above the spine.

We first consider the case $(\alpha_L, \alpha_R) = (1, 1)$, i.e., P_a is contained in a ↱-blocker and P_b is contained in a ↲-blocker. Let S_a and S_b be the blocker sequences starting at X_a and X_b, respectively. Observe that either S_a and S_b both end at X_a, or both end at X_b, or S_a ends at X_a and S_b ends at X_b. In the first two cases, there are no free spine edges, and in the third case, there is exactly one free spine edge X_cX_{c+1}, $a \leq c < b$, which can be seen by considering the blocker sequence starting at X_{a+1}. Applying Lemma 15 therefore concludes the proof in all those subcases.

We now consider the case $(\alpha_L, \alpha_R) = (0, 2)$, i.e., P_a and P_b are both contained in a ↲-blocker. Let X_k be the endpoint of the blocker starting at X_a. From Corollary 14, we obtain that $k < a$, i.e., the blocker sequence starting at X_a must end at X_0, enclosing all spine edges X_iX_{i+1}, $0 \leq i \leq r$. Applying Lemma 15 again completes the proof.

Case $\alpha = 3$**:** We only need to consider the cases $(\alpha_L, \alpha_R) = (1, 2)$ and $(\alpha_L, \alpha_R) = (0, 3)$. Let P_a, P_b, P_c, $a < b < c$, be the three points above the spine.

We first consider the case $(\alpha_L, \alpha_R) = (1, 2)$, i.e., P_b, P_c are both contained in a ↲-blocker. Let X_k be the endpoint of the blocker starting at X_b. From Corollary 14, we obtain that $k < b$, i.e., the blocker sequence starting at X_b must end at X_a, together with the blocker sequence starting at X_a, and both enclose all spine edges X_iX_{i+1}, $0 \leq i \leq r$. Consequently, we are done with the help of Lemma 15.

We now consider the case $(\alpha_L, \alpha_R) = (0, 3)$, i.e., all three points P_a, P_b, P_c are contained in a ↲-blocker. Corollary 14 implies that there are at least $2(\alpha_R - 1) = 4$ points P_i above the spine, a contradiction.

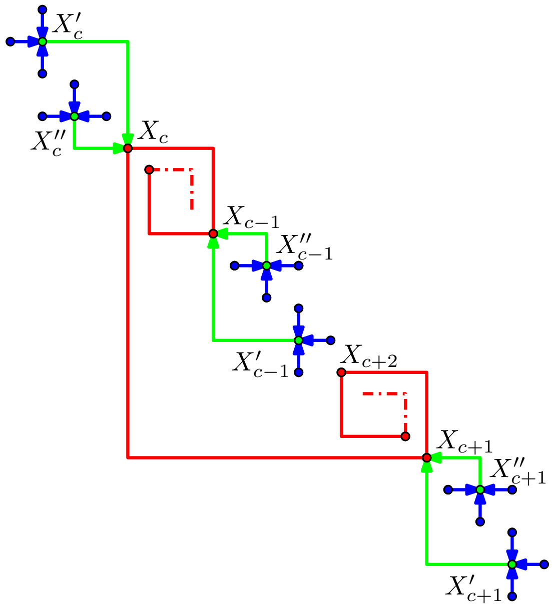

Figure 13: Illustration of Lemma 16.

Case $\alpha = 4$: We only need to consider the cases $(\alpha_L, \alpha_R) = (2, 2)$, $(\alpha_L, \alpha_R) = (1, 3)$, and $(\alpha_L, \alpha_R) = (0, 4)$. Let P_a, P_b, P_c, P_d, $a < b < c < d$, be the four points above the spine.

If $(\alpha_L, \alpha_R) = (2, 2)$, then Corollary 14 shows that the blocker sequences starting at X_b and X_c cannot coexist: Specifically, the blocker sequence starting at X_b with a ⮣-blocker ends at X_i with $b < i \leq r+1$, and the blocker sequence starting at X_c with a ⮠-blocker ends at X_j with $0 \leq j < c$. This is a contradiction. Similarly, if $(\alpha_L, \alpha_R) = (1, 3)$, then Corollary 14 shows that the blocker sequences starting at X_a and X_b cannot coexist. If $(\alpha_L, \alpha_R) = (0, 4)$, then Corollary 14 implies that there are at least $2(\alpha_R - 1) = 6$ points P_i above the spine, a contradiction.

Case $\alpha > 4$: Corollary 14 shows that there are at least $2(\alpha_L - 1) + 2(\alpha_R - 1) = 2\alpha - 4$ points P_i above the spine, which is a contradiction, as $2\alpha - 4 > \alpha$ for $\alpha > 4$.

4.2 Case 2: X_0X_1 is an ∟-edge

Throughout this section, we assume that X_0X_1 is an ∟-edge. Lemma 10 and the cyclic order of neighbors around each of the vertices X_i, $i = 0, \ldots, r+1$, now enforce a particular shape of all tree edges that connect two degree-4 vertices, as captured by the following lemma; see Figure 13.

Lemma 16. *For $i = 0, \ldots, r$, the vertex X_i is left of X_{i+1} and both are connected by a ∟-edge if i is even, and the vertex X_i is right of X_{i+1} and both are connected by a ¬-edge if i is odd. Moreover, for $i = 1, \ldots, r$,*

- *the vertices X'_i and X_i are connected by an ⬎-edge if i is even, and they are connected by an ⬑-edge if i is odd;*
- *the vertices X''_i and X_i are connected by an ↳-edge if i is even, and they are connected by an ↰-edge if i is odd;*

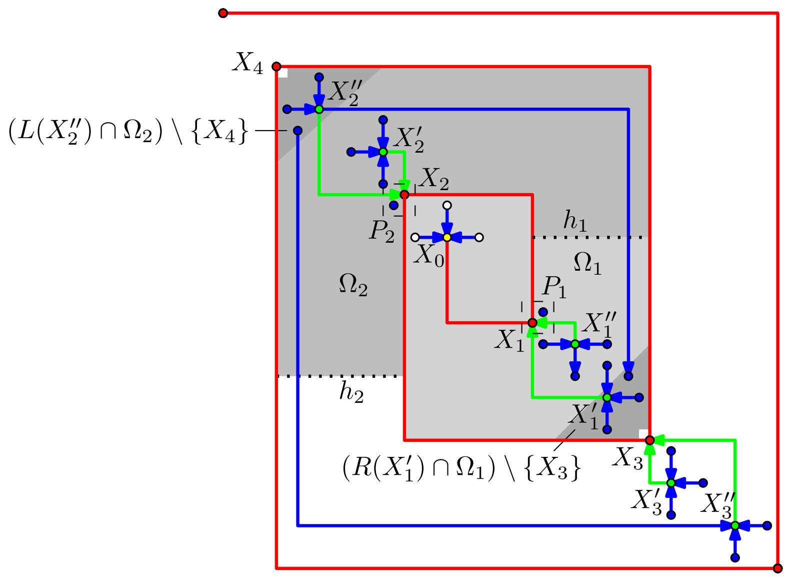

Figure 14: Illustration of the proof of Theorem 6 in Case 2.

- *the three edges directed from the leaves towards the vertex X_0 form a* [symbol]*, and the three edges directed from the leaves towards X_i' and X_i'' form a* [symbol] *or* [symbol]*, respectively, if i is even, and a* [symbol] *or* [symbol] *if i is odd.*

We define the *length* of a spine edge X_iX_{i+1}, $0 \leq i \leq r$, in the embedding as the number of boxes in the $(2,\ldots,2)$-staircase between its endpoints plus 1. For instance, if it connects two neighboring boxes, then its length is 1. By Lemma 16, there is a unique longest spine edge X_cX_{c+1}, $0 \leq c \leq r$, and the two length sequences of the edges X_iX_{i+1} for $i = c, c+1, \ldots, r$ and $X_{i+1}X_i$ for $i = c, c-1, \ldots, 0$ are strictly decreasing, i.e., each of the two corresponding parts of the spine spirals into itself in counterclockwise or clockwise direction, respectively, as shown in Figure 13. By the requirement that $r \geq 10$, the longer of these two sequences consists of at least 6 spine edges, and by symmetry we may assume that it is the latter one, i.e., the initial part of the spine looks as shown in Figure 14.

For $i \in \{1, 2\}$, we let h_i denote the horizontal line segment between the vertical segments of the spine edges X_iX_{i+1} and $X_{i+2}X_{i+3}$, and let Ω_i denote the region enclosed by the spine and this segment; see the figure. One of the leaves of the tree T_r^* must be mapped to the point P_1, which lies in the same box as X_1. This can only be the leaf adjacent to X_2'' via a ⌝-edge, or the leaf adjacent to X_1' via a ⌜-edge, or the leaf adjacent to X_1'' via a ⌞-edge. In the last two cases, the leaf adjacent to X_2'' via a ⌝-edge must reach into the region $(R(X_1') \cap \Omega_1) \setminus \{X_3\}$ or into the region $(R(X_1'') \cap \Omega_1) \setminus \{X_3\}$, respectively. This is because this region contains an even number of points, and therefore an even number of tree vertices must be mapped to them. In any case, the edge leaving X_2'' to the right must reach into Ω_1. Consequently, the leaf adjacent to X_3'' via a ⌞-edge must reach into the region $(L(X_2'') \cap \Omega_2) \setminus \{X_4\}$, in order to map an even number of tree vertices to this region. However, as none of the leaves of X_2' can connect to P_2, which lies in the same box as X_2, no vertex is mapped to P_2, a contradiction.

This completes the proof of Theorem 6.

5 Computer-based proofs of Theorems 1 and 3

We implemented a C++ program to test whether a given (unordered or ordered) tree admits an L-shaped embedding in a given set of points. Our algorithm recursively embeds vertices and edges in all possible ways until either a crossing occurs or a valid drawing is obtained.

Each point set is represented by a permutation, which captures the y-coordinates of the points from left to right. Those permutations are generated in lexicographic order using the C++ standard library function `next_permutation`. When embedding unordered trees, only point sets that are non-isomorphic up to rotation and mirroring need to be tested, by considering only the lexicographically smallest permutation obtained by those operations. Similarly, when embedding ordered trees, we factor our point sets that are isomorphic up to rotation (but not mirroring).

The list of all non-isomorphic unordered and ordered trees was generated with SageMath [S$^+$18], using the integrated nauty graph generator [MP14], and then loaded by the C++ program.

When testing ordered trees, we only need to test trees that admit more than one way to cyclically order the neighbors of all vertices, as otherwise the tree is equivalent to the corresponding unordered tree. Here we consider two ordered trees the same if they differ only in changing the orientation of all cyclic orders from clockwise to counterclockwise or vice versa, which corresponds to mirroring the embedding.

As pairs of trees and point sets can be tested independently, we parallelized our computations; see Table 1. The source code of all those programs is available online [MS].

Table 1: Number of non-isomorphic point sets and unordered/ordered trees with maximum degree 4 up to $n \leq 12$, and the computation times of our C++ program. The times marked with * are the sum of parallelized computations on 16 cores.

n	point sets OEIS/A903	unordered trees OEIS/A602	CPU time	point sets OEIS/A263685	ordered trees	CPU time
4	7	2		9	2	
5	23	3		33	3	
6	115	5		192	5	
7	694	9		1.272	10	
8	5.282	18	< 1 sec	10.182	21	< 1 sec
9	46.066	35	9 sec	90.822	48	21 sec
10	456.454	75	7 min	908.160	120	21 min
11	4.999.004	159	12 hours	9.980.160	312	64 hours*
12	59.916.028	355	84 days*	119.761.980	864	—

6 Further non-embeddable examples

In this section, we present further pairs of (unordered) n-vertex trees and sets of n points for $n = 13, 14, 16, 17, 18, 19, 20$, which do not admit an L-shaped embedding. The trees T_n are obtained as subtrees of the tree shown in Figure 15, by taking the subgraph induced by all unlabeled vertices and the vertices with labels $\leq n$. The corresponding point sets are encoded below in staircase notation. Note that all those staircase point sets have rotation and reflection symmetry and boxes of size at most 3. The fact that those instances do not allow an L-shaped embedding was established with computer help via a SAT solver, as described below.

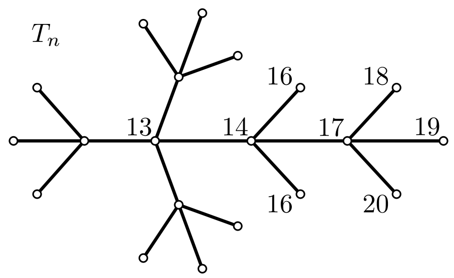

Figure 15: The 20-vertex tree T_{20}.

$n = 13$:

```
(1,1,2,2,1,2,2,1,1)
(1,1,3,1,1,1,3,1,1)
(2,2,2,1,2,2,2)
(2,3,1,1,1,3,2)
```

$n = 14$:

```
(1,1,2,1,2,2,1,2,1,1)
(2,2,1,2,2,1,2,2)
```

$n = 16$:

```
(1,3,1,1,1,2,1,1,1,3,1)
(1,3,2,1,2,1,2,3,1)
```

$n = 17$:

```
(1,1,3,1,1,3,1,1,3,1,1)
```

$n = 18$:

```
(1,1,2,1,1,1,2,2,1,1,1,2,1,1)
```

$n = 19$:

```
(1,1,3,1,1,1,3,1,1,1,3,1,1)
(1,1,3,1,2,3,2,1,3,1,1)
(1,1,3,2,1,3,1,2,3,1,1)
(2,3,1,1,1,3,1,1,1,3,2)
(2,3,1,2,3,2,1,3,2)
(2,3,2,1,3,1,2,3,2)
```

$n = 20$:

```
(1,1,2,1,1,1,2,2,2,1,1,1,2,1,1)
(1,1,2,1,2,2,2,2,2,1,2,1,1)
```

```
(1,1,2,2,1,2,2,2,1,2,2,1,1)
(2,2,1,1,1,2,2,2,1,1,1,2,2)
(2,2,1,2,2,2,2,2,1,2,2)
(2,2,2,1,2,2,2,1,2,2,2)
```

6.1 The SAT model

To test whether a given tree with vertex set $\{1, \ldots, n\}$ admits an L-shaped embedding in a given point set $\{P_1, \ldots, P_n\}$, we formulated a Boolean satisfiability problem that has a solution if and only if the tree admits an embedding in the point set.

Our SAT model has variables $x_{i,j}$ to indicate whether the vertex i is mapped to the point P_j, and for every edge ab in the tree a variable $y_{a,b}$ to indicate whether the edge is connected horizontally to a (otherwise it is connected vertically to a). The following constraints are necessary and sufficient to guarantee the existence of an L-shaped embedding:

- **Injective mapping from vertices to points:** Each vertex is mapped to a point, and no two vertices are mapped to the same point.
- **L-shaped edges:** For each edge ab of the tree, a is either connected horizontally or vertically to b. Figure 16(a) gives an illustration.
- **No overlapping edge segments:** For each pair of incident edges ab and ac, if b and c are mapped to the right of a, then a cannot be connected horizontally to both b and c. An analogous statement holds if b and c are both mapped to the left, above, or below a. Figure 16(b) gives an illustration.
- **No crossing edge segments:** For each pair of edges ab and cd, the vertices a, b, c, d must not be mapped so that segments cross. More specifically, for each four points p, q, r, s (to which a, b, c, d may map), there are at most four cases that have to be forbidden in the mapping, depending on the relative position of p, q, r, s. Figures 16(c) and 16(d) give an illustration.

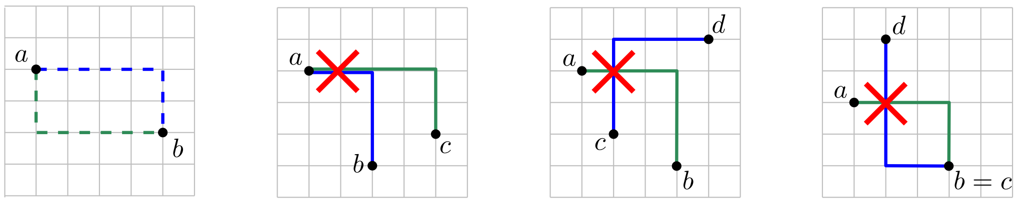

(a) (b) (c) (d)

Figure 16: Illustration of the constraints of the SAT model.

The resulting CNF formula thus has $\Theta(n^2)$ variables and $\Theta(n^4)$ clauses. Our Python program that creates a SAT instance for a given pair of tree and staircase point set is available online [MS]. We used the SAT solver PicoSAT [Bie08], which allows enumeration of all solutions. We also made use of pycosat, which provides Python bindings to PicoSAT.

7 Open problems

We currently do not know of any infinite family of (unordered) trees which do not always admit an L-shaped embedding. However, we conjecture that the instance in Figure 4 is such a family when considering the tree as unordered. Moreover, since all non-embeddable examples that we know are trees with pathwidth 2 (lobsters), it would be interesting to know whether trees with pathwidth 1 (caterpillars) always admit an L-shaped embedding. So far all known non-embeddable trees have maximum degree 4, so the question for trees with maximum degree 3 remains open [KS11, FHM+12, DGFF+13].

A more general class of embeddings are *orthogeodesic* embeddings, where the edges are drawn with minimal ℓ_1-length and consist of segments along the grid induced by the point set [KKRW10, DGFF+13, Sch15, BBHL16]. The best known bounds are due to Bárány et al. [BBHL16] who showed that every n-vertex tree with maximum degree 4 admits an orthogeodesic embedding in every point set of size $\lfloor 11n/8 \rfloor$. Unfortunately, our example T_{13} allows an orthogeodesic embedding in S_{13} (see Figure 17), so the question whether n points are always sufficient to guarantee an orthogeodesic embedding of any n-vertex tree [DGFF+13, BBHL16], also remains open.

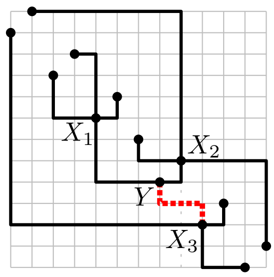

Figure 17: An orthogeodesic embedding of the tree T_{13} in the point set S_{13}. The only edge with two turns (not L-shaped) is drawn dotted.

Acknowledgements

Manfred Scheucher was partially supported by DFG Grant FE 340/12-1. We gratefully acknowledge the computing time granted by TBK Automatisierung und Messtechnik GmbH.

References

[AHS16] O. Aichholzer, T. Hackl, and M. Scheucher. Planar L-shaped point set embeddings of trees. In *Proc. 32nd European Workshop on Computational Geometry (EuroCG 2016)*, pages 51–54, 2016.

[BBHL16] I. Bárány, K. Buchin, M. Hoffmann, and A. Liebenau. An improved bound for orthogeodesic point set embeddings of trees. In *Proc. 31nd European Workshop on Computational Geometry (EuroCG 2015)*, pages 47–50, 2016.

[BCD+18] T. Biedl, T. M. Chan, M. Derka, K. Jain, and A. Lubiw. Improved bounds for drawing trees on fixed points with L-shaped edges. In *Graph drawing and network visualization*, volume 10692 of *Lecture Notes in Comput. Sci.*, pages 305–317. Springer, Cham, 2018.

[Bie08] A. Biere. PicoSAT essentials. *Journal on Satisfiability, Boolean Modeling and Computation (JSAT)*, 4:75–97, 2008.

[DGFF+13] E. Di Giacomo, F. Frati, R. Fulek, L. Grilli, and M. Krug. Orthogeodesic point-set embedding of trees. *Comput. Geom.*, 46(8):929–944, 2013.

[FHM+12] M. Fink, J.-H. Haunert, T. Mchedlidze, J. Spoerhase, and A. Wolff. Drawing graphs with vertices at specified positions and crossings at large angles. In *WALCOM: algorithms and computation*, volume 7157 of *Lecture Notes in Comput. Sci.*, pages 186–197. Springer, Heidelberg, 2012.

[KKRW10] B. Katz, M. Krug, I. Rutter, and A. Wolff. Manhattan-geodesic embedding of planar graphs. In *Graph drawing*, volume 5849 of *Lecture Notes in Comput. Sci.*, pages 207–218. Springer, Berlin, 2010.

[KS11] M. Kano and K. Suzuki. Geometric graphs in the plane lattice. In *Computational geometry*, volume 7579 of *Lecture Notes in Comput. Sci.*, pages 274–281. Springer, Cham, 2011.

[MP14] B. D. McKay and A. Piperno. Practical graph isomorphism, II. *J. Symbolic Comput.*, 60:94–112, 2014.

[MS] T. Mütze and M. Scheucher. Personal websites with source code of our programs. `http://page.math.tu-berlin.de/~muetze` and `http://page.math.tu-berlin.de/~scheucher/suppl/lshapes/`.

[MS18] T. Mütze and M. Scheucher. On L-shaped point set embeddings of trees: first non-embeddable examples. In *Proceedings of 26th International Symposium on Graph Drawing and Network Visualization (GD 2018)*, 9 pages. 2018.

[RS83] N. Robertson and P. D. Seymour. Graph minors. I. Excluding a forest. *J. Combin. Theory Ser. B*, 35(1):39–61, 1983.

[S+18] W. A. Stein et al. *Sage Mathematics Software (Version 8.1).* The Sage Development Team, 2018. `http://www.sagemath.org`.

[Sch15] M. Scheucher. Orthogeodesic point set embeddings of outerplanar graphs. Master's thesis, Graz University of Technology, 2015.